



Research article

Neurovascular toxicity of N-methyl-D-aspartate is markedly enhanced in the developing mouse central nervous system



Sudhakar Vadivelu^{a,*}, Kui Xu^a, Vanja Tolj^a, Rahul Rege^a, Lindsay Darkins^b, Karthik Vishwanath^b

^a Division of Neurosurgery, Cincinnati Children's Hospital Medical Center, Cincinnati, OH, United States

^b Department of Physics, Miami University, Oxford, OH, United States

HIGHLIGHTS

- Neural and vascular cells exhibit age dependent vulnerability after NMDA stroke in developing mice when compared to the aged mouse.
- Developmental vulnerability is similar to developmental vulnerability in postnatal rat after excitotoxic induced stroke.
- Cortical response to deep brain stroke can be directly evaluated with diffuse reflectance spectroscopy.
- Diffuse reflectance spectroscopy identifies post stroke progression non-invasively.

ARTICLE INFO

Article history:

Received 19 March 2017
Received in revised form 26 May 2017
Accepted 16 June 2017
Available online 19 June 2017

Keywords:

Cell death
Neurovascular coupling
Penumbra
Perfusion
Optical spectroscopy
Excitotoxicity

ABSTRACT

Penumbral perfusion is critical to brain viability. Proximal arterial occlusion and deep brain stroke has variable effect on cortical dysfunction. Cortical microvessel collaterals may be recruited and at times sufficient for partial parenchymal perfusion. Postnatal neural and endothelial cells are markedly vulnerable to glutamate excitotoxicity. Early vascular cell stress may promote partial protective neural preconditioning though postnatally a developmental window of the cerebral microvasculature may be particularly vulnerable to injury. We tested the hypothesis that postnatal NMDA excitotoxic injury, when cerebral endothelial cells' central energy source is via glycolysis, is age specific. Neurovascular responses of cortical viability were directly identified with diffuse reflectance patterns of perfusion properties in a non-invasive manner, over time. Histological evaluation for neural and vascular cytoarchitectonic abnormalities were evaluated 4–7 days post injury. Optical diffuse reflectance recordings were obtained at the injection site prior to, immediately after and 48 h post injury. Extent of neurovascular injury at the infarct zone was greatest at PND 5 and cortical perfusion responses identified with recordings of pattern change. These data further suggest excitotoxic injury to both neural and vascular cells, in vivo, can enhance CNS injury in the young and neuroprotective strategies may benefit from vascular directed therapies.

© 2017 Elsevier B.V. All rights reserved.

1. Introduction

Central nervous system injury early in life has profound effects on ongoing medical care, significant disability, and death. Age and topography are critical factors towards vulnerability of this injury and subsequent plasticity and regeneration that may ensue. Neonatal injury may be related to in utero growth restriction and inflammation, asphyxia, and hypoxic ischemic injury [16,17] and mechanistically in part due to neural and vascular impairment

[11,23,24]. Early vasculopathy has been reported as a key contributor to neurodevelopmental vulnerability and this is not solely due to acute vascular rupture. Abnormal bidirectional transport across the cerebral endothelial cells may lead to abnormal function of the accessory cells participating in a functional neurovascular unit [3]. Recognizing developmental cerebral vasculopathy has shed light on the stage specific risk of hemorrhagic vulnerability in the choroid plexus not only in utero but also postnatally and this may be related to energy requirements of the microvasculature [17]. Primary cell cultures of brain endothelial cells have demonstrated increased release of tissue plasminogen activator and gelatinases after glutamate excitotoxic challenge in the postnatal derived cells and in adult derived cells [14]. Furthermore, primary mouse derived neonatal endothelial cells augmented neonatal neurotoxicity under

* Corresponding author at: Neurosurgery and Radiology Cincinnati Children's Hospital Medical Center, 3333 Burnet Ave Cincinnati, OH 45229, United States.

E-mail address: sudhakar.vadivelu@cchmc.org (S. Vadivelu).

glutamate stress when compared to adult cell derivatives [4]. Alternatively, hypoperfusion in utero may lead to abnormal cerebral microvasculature that may alternatively precondition towards transient protection against excitotoxic vulnerability [2].

Glutamate, a principal excitatory amino acid, mediates several cellular interactions principally through agonists, NMDA, AMPA, and kainate. Abnormal accumulation leads to a cascade of events including excessive intracellular calcium and neuronal injury [6,18]. Neuronal susceptibility to hypoxic ischemic injury and also glutamate excitotoxicity changes during development [10]. Glutamate agonists contribute to variability in pathological changes alongside stage dependent vulnerability. For example, ibotenate induced injury in the developing brain demonstrates wide spread vulnerability in the postnatal mouse gray and white matter in comparison to adult staged mice [9]. When examining human stem cell transplant strategies in postnatal mouse models, quisqualic acid was injected intracerebrally to produce profound grey matter injury rather than white matter [13]. Clinically, developmental cortical abnormalities after injury occur and this corroborates injury involving both gray and white matter. Noninvasively following cortical development with the understanding of vascular involvement has been poorly understood. Recently optical spectroscopy has led to advances in continuous noninvasive imaging of parenchymal response to traumatic brain injury, ischemic injury, and oncologic progression [21]. Given the vulnerability of neonatal endothelial and neural cells to glutamate excitotoxicity, we test this stage dependent vulnerability in the developing mouse brain after direct NMDA injection and second tested the hypothesis that the cortical perfusion response could be identified noninvasively through optical spectroscopy.

2. Methods

2.1. NMDA injection

Intracerebral injections 20 nmol NMDA dissolved in 0.01 Tris, pH 7.4 performed in postnatal day (PND) 3, 5, 7, 15 and 75 nmol NMDA in PND 60–80 mice C57bl6/129 mice. Briefly, mice were anesthetized with ice, ketamine and xylazine. Stereotaxic injections were made through a burr hole created in the calvarium with a Hamilton syringe into the striatum (bregma, AP 2.5 mm, ML 2 mm, V 3 mm postnatal; AP 0.6 mm, ML 2 mm, V 4 mm) ($n = 4 - 5$ mice per age group). Needle was kept in target location for approximately 20 s to prevent leakage. All animals were sacrificed 4–7 days post injection for histological studies. Frozen sections were obtained for standard hematoxylin and eosin staining.

2.2. Histological assessment

Histological evidence of neural and vascular injury were identified and in proximity to the needle track in the ipsilateral hemisphere. This was compared to the contralateral hemisphere as a control and also sham controlled PBS injected age matched mice ($n = 2$ per age group). Quantitative analysis of lesion per age group were examined by cross sectional area of lesion size through a representative coronal section through the striatum and independent *t*-test performed for comparative analysis. Significance was determined less than 0.05.

2.3. Diffuse reflectance spectroscopy

Broadband diffuse reflectance spectra were obtained from mice using a fiber optical reflectance probe ($n = 15$). As described elsewhere [20], the optical system was formed by coupling a white-LED source providing illumination between 450 and 650 nm (LLS-Cool

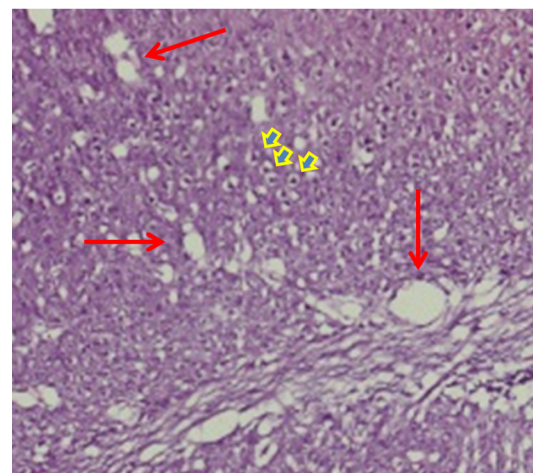
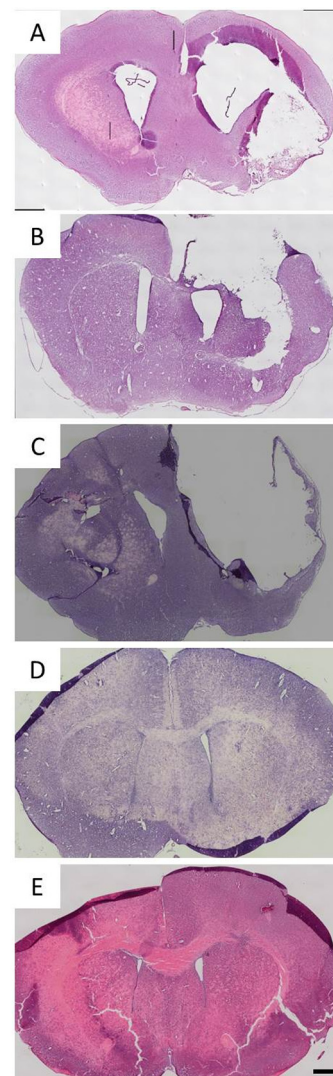


Fig 1. Hematoxylin and eosin stained coronal brain sections at the level of the needle tract and corpus striatum illustrating differential neurovascular toxicity produced by intrastriatal injection of specific glutamate agonist N-methyl-D-aspartate (NMDA) in the developing, (A) PND 3, (B) PND 5, (C) PND 7, (D) PND 15, and (E) adult mouse CNS. Postnatal mice received intrastriatal injection of 20nmol/0.05 ul NMDA and adult mice received 75nmol/1.5ul with sacrifice 4–7 days later). NMDA injections in immature mice resulted in tissue damage that was more extensive than damage by a similar injection of more than 3 times as much as NMDA injected in adult mice. Scale bar 1 mm. Inset of panel (B) demonstrating cortical necrosis and vacuolization both cortical and subcortical (periventricular).

White, Ocean Optics, Dunedin, FL) to a surface of interest via an optical fiber probe (R600-7-UV-VIS, Ocean Optics, Dunedin, FL) which detected the remitted diffuse reflectance from the surface using a spectrometer (USB4000, Ocean Optics, Dunedin, FL). The mean separation between each source-detector pair in the optical probe was 600 μm with the average tissue-depth sensed under the probe was expected to range between 300 μm and 500 μm . All reflectance scans were obtained in a darkened room.

For each animal, 100 diffuse reflectance scans were obtained by manually holding the optical probe for 3 s at the site of injection, along with a baseline reflectance measurement (obtained with the probe on a 99% white reflectance standard) and a reference reflectance from an optical phantom of known optical properties. Each scan was normalized by the baseline reflectance and then analyzed quantitatively using a photon transport model to extract the absorption and scattering coefficients of the tissue [8,15,22]. The tissue absorption coefficient was decomposed to yield the individual concentrations of oxygenated and deoxygenated hemoglobin ($[\text{HbO}_2]$ and $[\text{dHb}]$) which in turn were used to obtain the total tissue hemoglobin concentration as $[\text{THb}] = [\text{HbO}_2] + [\text{dHb}]$ and the percent vascular oxygen saturation as $\text{SO}_2 = 100 \times [\text{HbO}_2] / [\text{THb}]$. Reflectance scans were obtained from each animal before (pre) and immediately after (post) injection, while the probe was held in the same location ($n=8$). Measurements were also obtained 48 h post injections. The data in Fig. 2 show the derived optical parameters for each of the four representative animals, at the three times. The bars represent the average value of each parameter across the 100 scans, while the error bars represent the standard deviations. Optical measurements for Animal #8 were not obtained post injections. Figure three provides schematic representation of the real device with optical parameter determination values listed. Pictures of the real device and simplified utility on hand are shown.

3. Results

Neurovascular destruction after NMDA injection was assessed 4–7 days post injury in the ipsilateral hemispheres in comparison to contralateral hemispheres in each mouse. Area of injury was determined after identification of needle track and the parenchyma outlined. Within this perimeter of injury, cytoarchitectonic abnormalities including neuronal necrosis and vascular induced tissue vacuolization were qualitatively identified (Fig. 1). Quantitative assessment including cross-sectional area at this parenchymal perimeter and across 4–5 mice per age group was calculated. The proximal cross-sectional area after 20 nmol NMDA injection in PND 3 was 15.12 mm^2 , PND 5 was 22.5 mm^2 , PND 7 was 22.44 mm^2 , PND 15 was 2.86 mm^2 , and adult (PND 60–82) and after 75 nmol NMDA injection was 0.693 mm^2 . Neonatal susceptibility to NMDA cytotoxicity was greatest at PND 5 and PND 7 in comparison to the vulnerability of other age groups and this was 32.5 times the lesion size of the adult injury ($p < 0.001$).

For each mouse, 100 diffuse reflectance scans were obtained by manually holding the optical probe for approximately 3 s at the site of injection prior to needle penetration and after needle removal 2–10 min post injection and also at 48 h postinjury. Measurements of individual concentrations of oxygenated and deoxygenated hemoglobin were obtained to determine the total hemoglobin concentration within the parenchymal auricle tissue. The second measure of the neurovascular injured parenchyma was oxygen saturation at the same time points pre-and post injection and is well at 48 h post injection. The data represented in Fig. 2 demonstrates the derived percent change in optical parameters for two independent timed experiments ($n=4$ each for total $n=8$) at 3 separate measurements. PND 5 and adult mice were

assessed for diffuse reflectance spectroscopy properties in both control, sham, and NMDA injection mice ($n=15$). Representative PND 5 experimental mice #10 and 12 both demonstrated acute changes immediately postinjection in both oxygen saturation and total hemoglobin and by 48 h demonstrated elevated O₂ saturation and total hemoglobin greater than baseline. This was not too dissimilar to the response in the exposed skull but without needle insertion, representative PND 5 control mouse #8. However, the experimental mouse response was different from the representative sham mouse #9 with needle injection of PBS demonstrating reduced O₂ saturation without resolve and partial total hemoglobin response. Additionally, cumulative ($n=8$) percent change scores demonstrated increased total hemoglobin and reduced oxygen saturation (Fig. 2C).

4. Discussion

Developmental vulnerability to glutamate excitotoxicity beyond direct neural injury has recently been shown stressful to developing cerebral vascular cells. In fact, glycolysis as an energy source has been recently shown to be a predominant requirement in the postnatal day 5 age in comparison to later stages of development. Released factors from early aged endothelial cells derived from the cortical microvasculature augment glutamate distress to an already untowards neural injury. Glutamate induced elevation of tissue type plasminogen activator and matrix metallic proteinases is unique to neonatal brain microvasculature endothelial cells [7]. Elevated TPA has been shown to affect neuronal apoptosis and this may in part be due to MMP release [4]. Interestingly, therapeutic targeting directed against protease release from vascular cells may have a role in neuroprotection against hypoxic ischemic or excitotoxic neonatal brain injury [14]. Furthermore, glucose metabolism dependence of neonatal endothelial cells may be a critical determinant towards vascular extra cellular matrix remodeling in the progressive vulnerability of the neural parenchyma towards not only ischemia but also hemorrhagic stroke in an age dependent manner [16].

Use of NMDA excitotoxicity has been shown to be a reliable injury model in neonatal rat brain under stereotactic injection. Its role in developmental neurovascular injury is novel with growing evidence of NMDA-induced vulnerability of cerebral endothelial cells. In fact, we have previously demonstrated NMDA excitotoxic injury to the postnatal rat striatum and after transplantation of mouse embryonic stem cells, both neural and vascular cells differentiated suggesting injury to both neural and vascular cells [19]. Here, in this study, we characterized a developmental mouse model of targeted ischemic stroke that's critical to stage dependent vulnerability of immature cerebral microvasculature and neural development. We then employed a novel noninvasive tissue characterization of parenchymal perfusion properties, total hemoglobin and oxygen saturation of the injured cortex ipsilateral to the deep brain excitotoxic injury. Despite dramatic ipsilateral excitotoxic injury at 4–7 days post injection in the striatal territory, two days post injury was sufficient time to demonstrate early cortical parenchymal patterns of response different to sham control mice. Fluctuations in cortical parenchymal perfusion properties in experimental postnatal mice were not grossly observed in the adult experimental mice (unpublished observations). The partial return of total hemoglobin and oxygen saturation is not clearly discernable from either early commencement return of tissue repair or the beginning of a hyperemic response with further delayed injury. The histological evidence of significant cross sectional area damage including significant cortical disruption collateral microvascular recruitment, hyperemic response within ensuing insult progression, or cortical spreading depressions [5]. Not all mice are capable

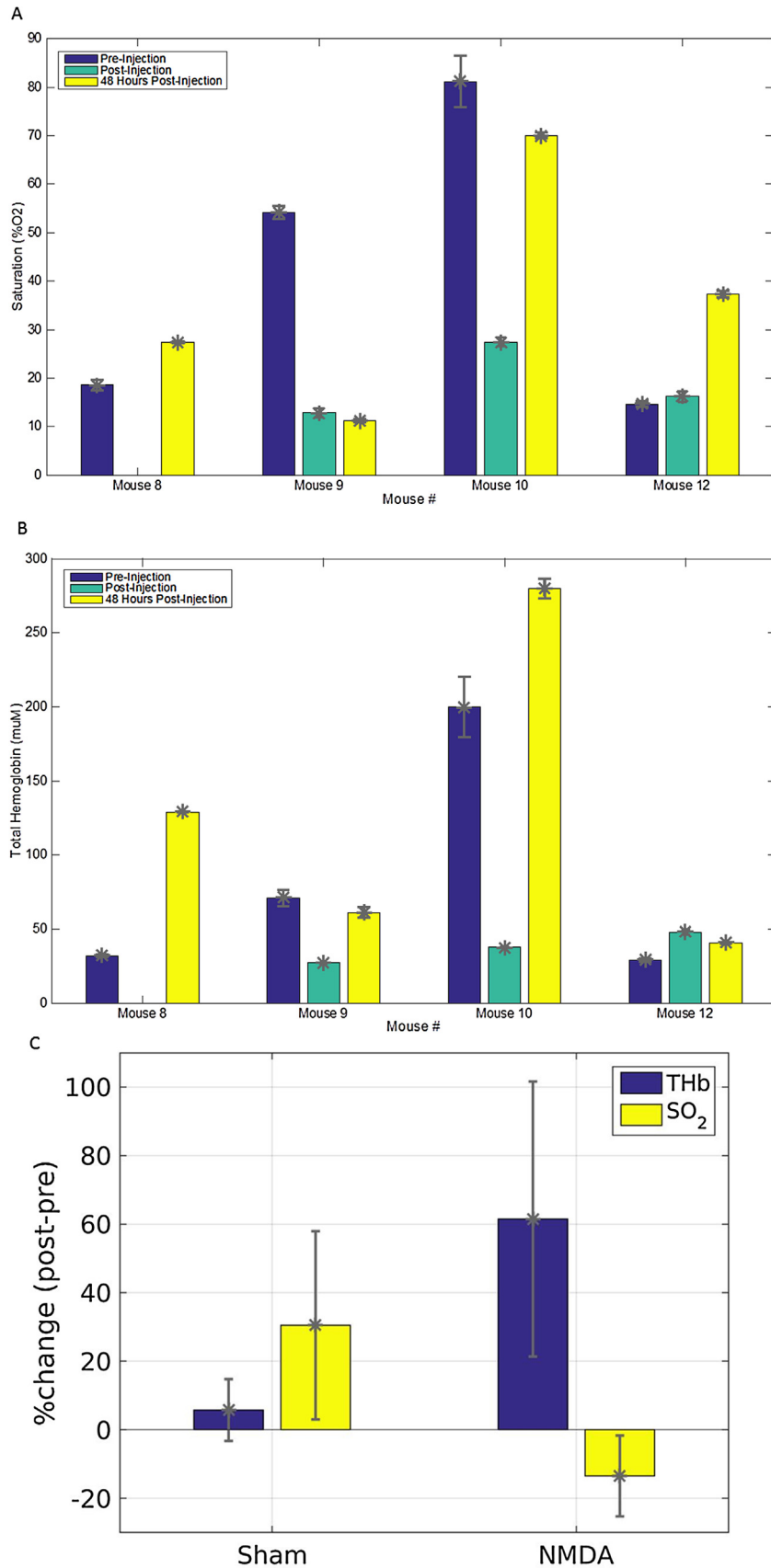


Fig. 2. Direct cortical parenchymal responses post striatal injury recorded with extracted optical parameters of total hemoglobin (Fig A) and oxygen saturation (Fig B) for the animals measured. Bars represent mean values of each parameter averaged across 100 repeated scans while error bars are standard deviations.

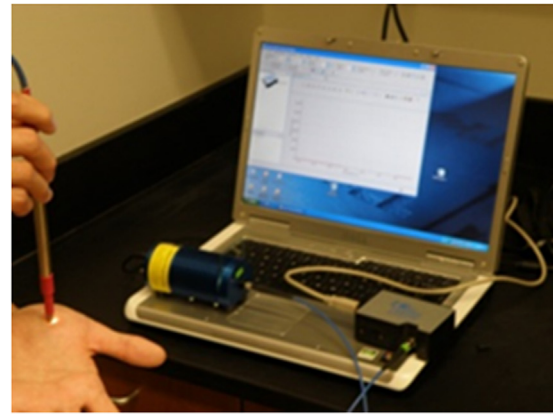
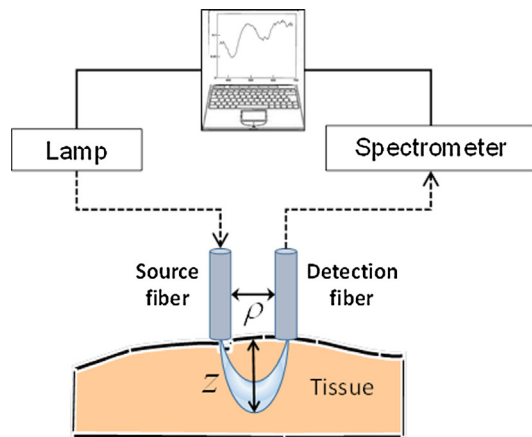


Fig. 3. The figure shows the schematic functioning of the DRS system and some photographs of the real device in use. The optical fiber is a Y-type probe, i.e. has one common end and two legs. One end of a leg is connected to the light source (typically a broadband lamp or LED) and delivers light to the surface of interest at the other end. This light enters the tissue, is scattered (or absorbed) by it and reaches the detector fiber placed some distance (ρ) away from the source-fiber. This source-detector distance determines how the depth sensitivity of the light in the tissue (z). For our studies here, $\rho = 600$ μm , giving an average depth sensitivity of 400–500 μm under the surface.

of eliciting collateral microcirculatory recruitment and this may be similar to protective responses seen clinically with higher prevalence of children with radiographic evidence of vasospasm without clinical sequelae than adults who are more likely to have clinical compromise when radiographic vasospasm is identified based largely on sufficient pediatric collateral microcirculatory responses ([12], Skoch et al. 2017 manuscript submitted). Diffuse reflectance spectroscopy used here has been shown with preliminary evidence to be useful for oncologic tissue, traumatic injury, and adult stroke models [5,21]. Hemoglobin and delivery of oxygen glucose are critical and likely predominate at the PND5 age glycolysis dominance at this time point. Our results demonstrate age dependent vulnerability and DRS optometrics may noninvasively identify hemodynamic responses that occur concomitant to metabolic and anatomic derangement. This agrees with recent evidence of DRS utility in closed head injury models and acute cerebral total hemoglobin and oxygen saturation responses [1,25]. Data reported here alongside this early literature suggests utility for translational studies identifying human perinatal stroke injury particularly addressing cortical injury progression and viability (Fig. 3).

Novel temporal evaluation of DRS technology in stroke evolution was assessed using a consistent NMDA excitotoxic injury model. Though optical spectroscopy given its translational, inexpensive, and portable application is subject to intermouse variability despite angled application to stereotaxic identified cortical sites, factors including wound healing, brain shift, systemic CO₂, O₂ and arterial blood pressure may affect optical responses. The optical signals are collected by holding the common leg of the optical probe at a site of interest (i.e. atop the scalp of the animal here) and collecting the diffusely reflected light. The probe was held at the site of NMDA injections and 100 scans acquired just before NMDA injection and 100 scans just after. The reflectance data collected would be expected to be impacted due to injury at the injection site as well as due to changes in blood flow and oxygenation in the cortical surface.

5. Conclusion

This study shows that postnatal cerebrum are particularly vulnerable to NMDA excitotoxic challenge. This developmental window demonstrates neural and vascular involvement in vivo and that distal parenchymal function responses to injury over time may be directly assessed by recording non-invasively cerebral perfusion parameters of oxygen saturation and total hemoglobin. These data

further suggest excitotoxic injury to both neural and vascular cells, in vivo, can enhance central nervous system injury in the young and neuroprotective strategies may benefit from vascular directed therapies during this developmental window.

References

- [1] D. Abookasis, B. Volkov, A. Shochat, I. Kofman, Noninvasive assessment of hemodynamic and brain metabolism parameters following closed head injury in a mouse model by comparative diffuse optical reflectance approaches, *Neurophotonics* 3 (2016) 025003.
- [2] J. Catteau, J.I. Gernet, S. Marret, H. Legros, P. Gressens, P. Leroux, V. Laudenbach, Effects of antenatal uteroplacental hypoperfusion on neonatal microvascularisation and excitotoxin sensitivity in mice, *Pediatr. Res.* 70 (2011) 229–235.
- [3] S. Guo, Y. Zhou, C. Xing, J. Lok, A.T. Som, M. Ning, X. Ji, E.H. Lo, The vasculome of the mouse brain, *PLoS One* 7 (2012) e52665.
- [4] V.J. Henry, M. Lecointre, V. Laudenbach, C. Ali, R. Macrez, A. Jullienne, V. Berezowski, P. Carmeliet, D. Vivien, S. Marret, B.J. Gonzalez, P. Leroux, High t-PA release by neonate brain microvascular endothelial cells under glutamate exposure affects neuronal fate, *Neurobiol. Dis.* 50 (2013) 201–208.
- [5] P.B. Jones, H.K. Shin, D.A. Boas, B.T. Hyman, M.A. Moskowitz, C. Ayata, A.K. Dunn, Simultaneous multispectral reflectance imaging and laser speckle flowmetry of cerebral blood flow and oxygen metabolism in focal cerebral ischemia, *J. Biomed. Opt.* 13 (2008) 044007.
- [6] J.Y. Koh, B.J. Gwag, D. Lobner, D.W. Choi, Potentiated necrosis of cultured cortical neurons by neurotrophins, *Science* 268 (1995) 573–575.
- [7] H. Legros, S. Launay, B.D. Roussel, A. Marcou-Labarre, S. Calbo, J. Catteau, P. Leroux, O. Boyer, C. Ali, S. Marret, D. Vivien, V. Laudenbach, Newborn- and adult-derived brain microvascular endothelial cells show age-related differences in phenotype and glutamate-evoked protease release, *J. Cereb. Blood Flow Metab.* 29 (2009) 1146–1158.
- [8] J. Malsan, R. Gurjar, D.E. Wolf, K. Vishwanath, Extracting Optical Properties of Turbid Media Using Radially and Spectrally Resolved Diffuse Reflectance, *SPIE Photonics West*, SPIE, San Francisco, CA, 2014 (pp. Paper 8936–8940).
- [9] S. Marret, R. Mukendi, J.F. Gadiuseux, P. Gressens, P. Evrard, Effect of ibotenate on brain development: an excitotoxic mouse model of microgyria and posthypoxic-like lesions, *J. Neuropathol. Exp. Neurol.* 54 (1995) 358–370.
- [10] J.W. McDonald, F.S. Silverstein, M.V. Johnston, Neurotoxicity of N-methyl-D-aspartate is markedly enhanced in developing rat central nervous system, *Brain Res.* 459 (1988) 200–203.
- [11] P.S. McQuillen, D.M. Ferriero, Selective vulnerability in the developing central nervous system, *Pediatr. Neurol.* 30 (2004) 227–235.
- [12] D.L. Mofatkhar, H.J. Cooke, N.U. Fullerton, M.R. Ko, J.A. Amans, C.F. Narvid, R.T. Dowd, V.V. Higashida, Extent of collateralization predicting symptomatic cerebral vasospasm among pediatric patients: correlations among angiography, transcranial Doppler ultrasonography, and clinical findings, *J. Neurosurg. Pediatr.* 15 (2015) 282–290.
- [13] D. Mueller, M.J. Shablott, H.E. Fox, J.D. Gearhart, L.J. Martin, Transplanted human embryonic germ cell-derived neural stem cells replace neurons and oligodendrocytes in the forebrain of neonatal mice with excitotoxic brain damage, *J. Neurosci. Res.* 82 (2005) 592–608.
- [14] P.L. Omouendze, V.J. Henry, B. Porte, N. Dupre, P. Carmeliet, B.J. Gonzalez, S. Marret, P. Leroux, Hypoxia-ischemia or excitotoxin-induced tissue plasminogen activator- dependent gelatinase activation in mice neonate brain microvessels, *PLoS One* 8 (2013) e71263.

- [15] G.M. Palmer, N. Ramanujam, Monte Carlo-based inverse model for calculating tissue optical properties. Part I: Theory and validation on synthetic phantoms, *Appl. Opt.* 45 (2006) 1062–1071.
- [16] B. Porte, C. Chatelain, J. Hardouin, C. Derambure, Y. Zerdoumi, M. Hauchecorne, N. Dupre, S. Bekri, B. Gonzalez, S. Marret, P. Cosette, P. Leroux, Proteomic and transcriptomic study of brain microvessels in neonatal and adult mice, *PLoS One* 12 (2017) e0171048.
- [17] B. Porte, J. Hardouin, Y. Zerdoumi, C. Derambure, M. Hauchecorne, N. Dupre, A. Obry, T. Lequerre, S. Bekri, B. Gonzalez, J.M. Flaman, S. Marret, P. Cosette, P. Leroux, Major remodeling of brain microvessels during neonatal period in the mouse: a proteomic and transcriptomic study, *J. Cereb. Blood Flow Metab.* 37 (2017) 495–513.
- [18] F.S. Silverstein, R. Chen, M.V. Johnston, The glutamate analogue quisqualic acid is neurotoxic in striatum and hippocampus of immature rat brain, *Neurosci. Lett.* 71 (1986) 13–18.
- [19] S. Vadivelu, M.M. Platik, L. Choi, M.L. Lacy, A.R. Shah, Y. Qu, T.F. Holekamp, D. Becker, D.I. Gottlieb, J.M. Giddy, J.W. McDonald, Multi-germ layer lineage central nervous system repair: nerve and vascular cell generation by embryonic stem cells transplanted in the injured brain, *J. Neurosurg.* 103 (2005) 124–135.
- [20] K. Vishwanath, K. Chang, D. Klein, Y. Deng, V.C. Chang, N. Ramanujam, Portable, fiber-Based diffuse reflection spectroscopy (DRS) systems for estimating tissue optical properties, *Appl. Spectrosc.* 65 (2011) 206–215.
- [21] K. Vishwanath, K. Chang, D. Klein, Y.F. Deng, V. Chang, J.E. Phelps, N. Ramanujam, Fiber-Based portable, diffuse reflection spectroscopy (DRS) systems for estimating tissue optical properties, *Appl. Spectrosc.* 62 (2011) 206–215.
- [22] K. Vishwanath, D. Klein, K. Chang, T. Schroeder, M.W. Dewhirst, N. Ramanujam, Quantitative optical spectroscopy can identify long-term local tumor control in irradiated murine head and neck xenografts, *J. Biomed. Opt.* 14 (2009) 054051.
- [23] J.J. Volpe, Brain injury in premature infants: a complex amalgam of destructive and developmental disturbances, *Lancet Neurol.* 8 (2009) 110–124.
- [24] J.J. Volpe, The encephalopathy of prematurity? brain injury and impaired brain development inextricably intertwined, *Semin. Pediatr. Neurol.* 16 (2009) 167–178.
- [25] R.H. Wilson, K. Vishwanath, M.-A. Mycek, Optical methods for quantitative and label-free sensing in living human tissues: principles, techniques, and applications, *Adv. Phys.: X TBD* (2016).